

1

2

3

4 **A high-throughput assay to identify robust inhibitors**  
5 **of dynamin GTPase activity**

6

7

8 **Aparna Mohanakrishnan<sup>1</sup>, Triet Vincent M. Tran<sup>1</sup>, Meera Kumar<sup>2</sup>, Hong Chen<sup>3</sup>,**  
9 **Bruce A. Posner<sup>3</sup>, and Sandra L. Schmid<sup>1\*</sup>**

10

11

12 <sup>1</sup> Department of Cell Biology, UT Southwestern Medical Center, Dallas, TX USA

13 <sup>2</sup> BellBrook Labs, Madison, WI USA

14 <sup>3</sup> Department of Biochemistry, UT Southwestern Medical Center, Dallas, TX USA

15

16

17 \* Corresponding author

18 Email: [sandra.schmid@utsouthwestern.edu](mailto:sandra.schmid@utsouthwestern.edu) (SLS)

## 19 **Abstract**

20           Clathrin-mediated endocytosis is the major pathway by which cells internalize  
21 materials from the external environment. Dynamin, a large multidomain GTPase, is a  
22 key regulator of clathrin-mediated endocytosis. It assembles at the necks of invaginated  
23 clathrin-coated pits and, through GTP hydrolysis, catalyzes scission and release of  
24 clathrin-coated vesicles from the plasma membrane. Several small molecule inhibitors  
25 of dynamin's GTPase activity, such as Dynasore and Dyngo-4a, are currently available,  
26 although their specificity has been brought into question. Previous screens for these  
27 inhibitors measured dynamin's stimulated GTPase activity due to lack of sufficient  
28 sensitivity, hence the mechanisms by which they inhibit dynamin are uncertain. We  
29 report a highly sensitive fluorescence-based assay capable of detecting dynamin's  
30 basal GTPase activity under conditions compatible with high throughput screening.  
31 Utilizing this optimized assay, we conducted a pilot screen of 8000 compounds and  
32 identified several "hits" that inhibit the basal GTPase activity of dynamin-1. Subsequent  
33 dose-response curves were used to validate the activity of these compounds.  
34 Interestingly, we found neither Dynasore nor Dyngo-4a inhibited dynamin's basal  
35 GTPase activity, although both inhibit assembly-stimulated GTPase activity. This assay  
36 provides the basis for a more extensive search for robust dynamin inhibitors.

37

## 38 Introduction

39           Dynamamin is a large multidomain GTPase known for its role in catalyzing  
40 membrane fission in clathrin-mediated endocytosis (CME) [1-3]. It consists of five  
41 functional domains: the N-terminal GTPase domain (G domain); the middle domain and  
42 the GTPase effector domains (GEDs), which together form the stalk of dynamamin; a  
43 pleckstrin homology (PH) domain; and the C-terminal proline- and arginine-rich domain  
44 (PRD), which interacts with many SH3 domain-containing proteins [4]. Dynamamin  
45 assembles at the necks of invaginated clathrin-coated pits and catalyzes scission and  
46 release of clathrin-coated vesicles from the plasma membrane. Dynamamin is recruited to  
47 nascent coated pits in its unassembled state and also plays a regulatory role during the  
48 early stages of CME [5-7].

49           Most GTPase family members that function as regulatory proteins do so by  
50 switching between GTP-bound 'active' conformations and GDP-bound 'inactive' states.  
51 Their intrinsic GTP hydrolysis rates are slow, and rate-limited by the exchange of tightly-  
52 bound GDP for GTP. These two steps in the GTP hydrolytic cycle are regulated by  
53 GTPase activating proteins (GAPs) and GTP exchange factors (GEFs), respectively. In  
54 this regard, dynamamin is an atypical GTPase as it has a low affinity for GTP (2-5  $\mu\text{M}$ ), a  
55 high rate of GDP dissociation ( $\sim 60\text{-}90\text{ s}^{-1}$ ), and a comparatively robust and measurable  
56 basal rate of GTP hydrolysis ( $\sim 1\text{ min}^{-1}$  at  $37^\circ\text{C}$ ) [8]. However, upon self-assembly,  
57 interactions between G domains can stimulate GTPase activity *in trans* [9]. *In vivo*,  
58 dynamamin self-assembles into short helical structures that surround the necks of deeply  
59 invaginated coated pits. *In vitro*, dynamamin assembles into long helical arrays around lipid  
60 nanotubes whereby its GTPase activity is stimulated  $> 100$ -fold [10]. Dynamamin's GTPase

61 activity can also be stimulated, albeit to a lesser extent, through interactions with  
62 divalent SH3 domain containing partners such as Grb2 [11,12] or under low salt  
63 conditions that favor dynamin self-assembly [13].

64         Given its importance for clathrin-mediated endocytosis, coupled to the fact that it  
65 is one of the few enzymes known to be required for CME, small molecule inhibitors of  
66 dynamin's GTPase activity have been sought as potentially powerful tools for studying  
67 CME. Indeed, several chemical inhibitors of dynamin have been reported and are  
68 commercially available, including Dynasore [14,15] and its structural derivative, Dyngo-  
69 4a [14,15]. However, recent findings have brought into question the specificity of these  
70 compounds. For example, Dynasore and Dyngo-4a continue to inhibit endocytosis in  
71 triple dynamin-1, 2, and 3 knockout cells, thus revealing potential off-target effects [16].  
72 These off-target effects on endocytosis may reflect their reported ability to perturb  
73 plasma membrane cholesterol levels [17] and destabilize actin filaments [16]. Recently,  
74 Dynasore was shown to impair VEGFR2 signaling in an endocytosis-independent  
75 manner [18]. Based on the clear evidence for dynamin-independent, off-target effects of  
76 these compounds, there remains a need to develop more specific and robust dynamin  
77 inhibitors.

78         Previous screens for small molecule inhibitors of dynamin's GTPase activity were  
79 based on the detection of released phosphate using a malachite green colorimetric  
80 assay. However, this assay lacks sufficient sensitivity to detect dynamin's basal  
81 GTPase activity, especially when measured at room temperature and at the low  
82 concentrations of dynamin and GTP practically needed for the design of a high-  
83 throughput assay. To circumvent this, previous high throughput screens measured

84 dynamin's stimulated GTPase activity either in the presence of GST-Grb2 [14,15] or  
85 with sonicated phosphatidylserine (PS) liposomes at low salt [14,15]. Dynasore, and by  
86 extension Dyngo-4a, was shown to be a noncompetitive inhibitor of dynamin's GTPase  
87 activity [14,15]. Hence its mechanism of action, which remains unknown, may reflect  
88 indirect effects on dynamin assembly or aggregation.

89 Here we report the optimization of a new, highly sensitive, and robust HTS-  
90 compatible assay to detect the basal GTPase activity of dynamin and its validation in a  
91 preliminary screen of 8000 compounds.

92

## 93 **Materials and methods**

### 94 **Dynamin expression, purification, and preparation**

95 Dynamin-1 (Dyn1) was expressed in Sf9 insect cells and purified by affinity  
96 chromatography, as previously described [19]. Protein aliquots were flash frozen in  
97 liquid nitrogen and stored in -80°C in 5% v/v glycerol. Prior to running assays, frozen  
98 aliquots of Dyn1 were thawed and centrifuged at 100,000 g for 15 minutes to remove  
99 any aggregates. Dyn1 concentration was determined by measuring its absorbance at  
100 280 nm with a UV/Vis spectrophotometer (Beckman Coulter Inc.) using a molar  
101 absorptivity coefficient of 73,800 M<sup>-1</sup> cm<sup>-1</sup>.

102

### 103 **Transcreener GDP fluorescence polarization assay**

104 The Transcreener<sup>®</sup> GDP FP (BellBrook Labs) assay is an immune-competition  
105 assay based on a mouse monoclonal antibody that selectively binds Alexa633-

106 conjugated GDP over GTP. The preformed Alexa633-GDP antibody complex is added  
107 at the end of the reaction, and the GDP generated displaces bound Alexa633  
108 fluorescent tracer, resulting in a decrease in its far-red fluorescence polarization (FP).  
109 The assay detects GDP production with high sensitivity at low substrate concentrations  
110 and has been used to develop an HTS compatible assay for the enzymatic activity of  
111 ARFGAP [20]. Stocks of 5 mM GTP, 10x Stop & Detect Buffer B, 400 nM GDP  
112 Alexa633 Tracer, and 3100 µg/mL GDP antibody were purchased from BellBrook Labs  
113 (Madison, WI). Assays were performed in Corning 384-well plates at room temperature.

114 All assays were conducted in the endpoint format, which measures total GDP  
115 production after 60 minutes of incubation at room temperature. The optimized reaction  
116 (total volume 15 µL) was initiated by adding 5 µL of GTP (3x stock of 30 µM, final  
117 concentration 10 µM) to wells containing 10 µL Dyn1 (1.5x stock, final concentration 50  
118 or 100 nM). Reactions were terminated after 60 minutes with the addition of 5 µL of  
119 GDP detection mixture (4x stock of 8 nM GDP Alexa633 Tracer, 40 mM HEPES, 80 mM  
120 EDTA, 0.04% Brij and 34.4 µg/mL GDP antibody). The plates were incubated for  
121 another 60 minutes, allowing the GDP antibody-GDP binding to reach equilibrium. The  
122 plate was then read for fluorescence polarization in millipolarization units (mP) using an  
123 EnVision multi-modal microplate reader (PerkinElmer, Inc.). The mP values of the  
124 reaction-containing wells were subtracted from those containing no enzyme to obtain  
125  $\Delta$ mP values. To convert the polarization data to GDP released, a standard curve  
126 representing 0 to 100% GDP conversion from 10 µM GTP was generated. Using  
127 GraphPad Prism, the  $\Delta$ mP values were fitted to the standard curve to obtain the total

128 GDP production. Importantly, the assay was insensitive to DMSO concentrations up to  
129 3%.

130

## 131 **8000-compound library screen**

132 A screen was performed using the optimized Transcreeper GDP FP assay on a  
133 diverse library subset of 8000 small molecule compounds, provided by the UT  
134 Southwestern HTS Core. For the HTS screen, the final concentration of Dyn1 in the  
135 reaction mixture was 50 nM. 0.3  $\mu$ L of compound in 100% DMSO (final concentration 10  
136  $\mu$ M compound, 2% DMSO) was added to the Dyn1 and pre-incubated for 30 minutes.  
137 Controls for the screen included reactions that lacked enzyme (positive control for  
138 inhibition) and uninhibited reactions containing only DMSO (negative control for  
139 inhibition), which were dispensed in single columns in each plate. Solutions were  
140 dispensed using automated liquid handling devices.

141

## 142 **Data analysis**

143 The primary screen data were analyzed using Genedata Screener<sup>®</sup> software.  
144 The Z' factors for the mock screen and the 8000-compound pilot screen were calculated  
145 using the equation below:

$$146 \quad Z' \text{ factor} = 1 - \frac{3(\sigma_{\text{positive control}} + \sigma_{\text{sample or negative control}})}{|\mu_{\text{positive control}} - \mu_{\text{sample or negative control}}|} \quad (1)$$

147 where  $\sigma_{\text{positive control}}$  is the standard deviation of the positive controls for inhibition, and  
148  $\sigma_{\text{sample or negative control}}$  is the standard deviation of the samples or negative controls for

149 inhibition, respectively.  $\mu_{\text{positive control}}$  is the mean of the positive control for inhibition, and  
150  $\mu_{\text{sample or negative control}}$  is the mean of the samples or neutral DMSO controls, respectively.

151 The samples were normalized by a two-point correction method using the  
152 equation below:

$$153 \quad \textit{Two point normalized values} = \frac{\textit{raw value}_{\textit{sample}} - \textit{median}_{\textit{total samples}}}{\textit{median}_{\textit{positive controls}} - \textit{median}_{\textit{total samples}}} \times 100 \quad (2)$$

154 where  $\text{median}_{\text{total samples}}$  is defined as the median of all library compound-containing  
155 reaction wells within the plate.

156 The two-point normalized activity values were adjusted using a correction factor  
157 to account for systematic errors within and across assay plates [21]. The correction  
158 factor of a well in a given plate is calculated using pattern detection algorithms that are  
159 proprietary to the Screener<sup>®</sup> software (Genedata, Inc.). The corrected activity values  
160 were then used to determine the robust Z (RZ) score with the following equation:

$$161 \quad \textit{Robust Z score} = \frac{\textit{normalized value of sample} - \textit{median of DMSO controls}}{\textit{robust STD of DMSO controls}} \quad (3)$$

162 where robust STD is the standard deviation calculated using the median of the DMSO  
163 controls (negative control for inhibition).

164 For the confirmation screen and dose response curves, the data were analyzed  
165 by normalizing the sample GDP released to the control GDP released using the  
166 following equation:

$$167 \quad \textit{normalized GTPase activity} = \frac{\textit{sample}_{\textit{GDP released}}}{\textit{control}_{\textit{GDP released}}} \times 100 \quad (4)$$

168

169 **Malachite green assay**



170 The lipid nanotube (NT)-stimulated malachite green assays were performed in  
171 96-well plates at 37°C. The final reaction consisted of 100 nM Dyn1, 25 µM GTP, and  
172 300 µM lipid nanotubes. The assay and reagent preparations were performed according  
173 to our published protocol [22]. All general chemicals were purchased from Sigma-  
174 Aldrich (St. Louis, MO). Compounds tested in the malachite green assay were  
175 purchased from Chembridge and ChemDiv (both located in San Diego, CA).

176

## 177 **Results**

### 178 **Optimization of a fluorescence polarization assay to detect** 179 **basal GTPase activity of dynamin**

180 Fluorescence polarization (FP) is a method that allows for rapid and quantitative  
181 analysis of diverse molecular interactions and enzyme activities [23]. Polarization  
182 measures the change in the molecular movement of the labeled species. It is the ratio of  
183 the difference between the vertical and horizontal components of the emitted light over  
184 their sum [20]. In recent years, FP has been successfully used in HTS of compound  
185 libraries to identify small molecule inhibitors of protein-protein interactions.

186 Bellbrook labs has developed an assay that detects GDP using a competitive FP  
187 immunoassay. GDP released upon hydrolysis of GTP by GTPases displaces a  
188 fluorescent tracer from the antibody, resulting in a decrease in polarization due to  
189 increased rotational mobility. The antibody has 140-fold specificity for GDP versus GTP,  
190 which allows sensitive measurement of GDP in the presence of excess GTP.

191 Given that the antibody used has a finite selectivity for GDP over GTP, it was necessary

192 to determine the optimal concentration of the Alexa-GDP antibody conjugate needed for  
193 maximum mP measured in the presence of 10, 100 and 500  $\mu\text{M}$  GTP, our initial  
194 substrate concentrations. For this purpose, the Alexa-GDP antibody conjugate was  
195 titrated into the reaction mixture containing GTP (10, 100 or 500  $\mu\text{M}$ ) and assay buffer  
196 (20 mM HEPES, 150 mM KCl, 1 mM EDTA, 1 mM EGTA and 1 mM DTT, pH 7.4). The  
197 data were fitted to a variable slope sigmoidal dose-response curve using GraphPad  
198 Prism (Fig 1A). From the titration curves, we determined the optimal GDP antibody  
199 concentrations to be 8.6, 81.5 and 405.5  $\mu\text{g}/\text{mL}$  for 10, 100 and 500  $\mu\text{M}$  GTP,  
200 respectively (highlighted data points in Fig 1A). These concentrations were chosen near  
201 signal saturation and represent a good compromise between sensitivity and maximal  
202 polarization value.

203 To convert  $\Delta\text{mP}$  to  $\mu\text{M}$  GDP released, we generated a standard curve by titrating  
204 increasing concentrations of GDP in the presence of GTP to mimic reaction conditions.  
205 The assay accurately measures GTP hydrolysis in the range of 0.05% to 10% of the  
206 substrate converted (Fig 1B).

207 To determine the optimal conditions for high throughput screening, we measured  
208  $\Delta\text{mP}$  for increasing concentrations of Dyn1 (0.3 nM to 5000 nM) at three different  
209 concentrations of GTP (10, 100, and 500  $\mu\text{M}$ ) (Fig 2A). These titrations established that  
210 50 nM Dyn1, assayed in the presence of 10  $\mu\text{M}$  GTP for 60 minutes, resulted in  
211 excellent signal-to-noise with high reproducibility. We further confirmed that, under  
212 these conditions, the basal rate of GTP hydrolysis by Dyn1 ( $\sim 0.04 \text{ min}^{-1}$  at 10  $\mu\text{M}$  GTP)  
213 was linear for 60 min (Fig. 2B). These results are consistent with assays performed at

214 room temperature and under low substrate concentrations. We chose 60 minutes to  
215 ensure that substrate consumption remained below 10%. Importantly, no signal was  
216 detected at any concentration of GTP when S45N mutant Dyn1, which is unable to bind  
217 GTP [24], was used as a negative control (Fig 2C). We further confirmed that under  
218 these conditions, GTPase activity is directly proportional to the concentration of Dyn1.  
219 Thus, there is no evidence of cooperativity and the assay measures the basal rate of  
220 GTP hydrolysis of unassembled Dyn1 (Fig 2D).

221

## 222 **Pilot screen, hit selection and validation**

223 We measured the robustness of the assay under our optimized HTS conditions  
224 to determine whether ‘hits’ could be identified with high confidence. mP values obtained  
225 from 15  $\mu$ L reactions after a 60-minute incubation with 50 nM Dyn1 and 0.3  $\mu$ L of 100%  
226 DMSO in the presence of 10  $\mu$ M GTP were compared to those lacking Dyn1 (Fig 3A).  
227 The average Z’ factor for the mock screen, which was calculated to be 0.56, indicated  
228 that the assay was sufficiently robust for screening purposes.

229 A pilot screen using an 8000-compound diversity subset of the chemical library at  
230 UT Southwestern was conducted using the optimized Transcreener GDP FP assay. The  
231 compounds were tested for their inhibitory effects on the Dyn1 GTPase activity at a  
232 concentration of 10  $\mu$ M.

233 Intrinsically fluorescent compounds, which alter total fluorescence intensity per  
234 well, were eliminated, as they would impact analysis. After careful analysis of the data,  
235 we identified 42 compounds with a robust Z score greater than 3 as primary hits (Fig  
236 3B).

237           These compounds were re-tested in a confirmation screen at three different  
238 concentrations to validate their inhibitory effects, yielding 4 promising compounds based  
239 on concentration-dependent inhibition. To confirm the inhibitory effects of the 4  
240 compounds, we conducted 11-point dose response curves, with concentrations ranging  
241 from 1 nM to 100  $\mu$ M (Fig 4A). The IC<sub>50</sub> values of these compounds ranged from < 1  $\mu$ M  
242 to > 50  $\mu$ M. We focused on compound 24 which had an IC<sub>50</sub> of 0.58  $\mu$ M.

243

## 244   **Secondary assay and comparison with Dynasore and Dyngo-**

### 245   **4a**

246           Compound 24 was compared with the two commercially available dynamin  
247 inhibitors, Dynasore and Dyngo-4a, in a dose-response assay measuring inhibition of  
248 basal GTPase activity under high salt (150 mM KCl) conditions. The concentration of  
249 inhibitors ranged from 1 nM to 100  $\mu$ M. As seen in Fig 4B, Dynasore and Dyngo-4a do  
250 not appear to inhibit basal GTPase activity even at high concentrations, in contrast to  
251 previous findings in which assays were performed under conditions that measure  
252 dynamin's stimulated, assembly-dependent GTPase activity [14,15]. Therefore, to more  
253 closely parallel previous studies we tested both commercial inhibitors in comparison to  
254 compound 24 for their effects on dynamin's stimulated GTPase activity. Assays were  
255 performed in the presence of PI(4,5)P<sub>2</sub>-containing lipid nanotubes (NT), whose diameter  
256 (~ 20 nm) resembles the neck of an invaginated coated pit [10], using the malachite  
257 green assay. Under these conditions (100 nM Dyn1, 300  $\mu$ M lipid nanotubes, 25  $\mu$ M  
258 GTP), both Dynasore and Dyngo-4a inhibited the NT-stimulated GTPase activity of

259 Dyn1 with IC<sub>50</sub> values of 83.5 and 45.4 μM, respectively, as compared to compound 24,  
260 which exhibited an IC<sub>50</sub> of 6.4 μM in this assay (Fig 4C).

261

## 262 **Discussion**

263 We have optimized a robust, high-throughput assay to measure the basal  
264 GTPase activity of unassembled Dyn1. This highly sensitive assay detects the release  
265 of low, nanomolar amounts of GDP and hence, accurately measures the intrinsic, basal  
266 rate of GTP hydrolysis, even at the low concentrations of dynamin and GTP necessary  
267 for HTS design and implementation. Previous high throughput screens using a less  
268 sensitive colorimetric malachite green assay to detect phosphate release were  
269 necessarily performed under conditions that stimulate dynamin's GTPase activity, i.e. in  
270 the presence of dimeric GST-Grb2, which presumably aggregates dynamin, or with  
271 sonicated PS liposomes in low salt.

272 Utilizing the Transcreener GDP FP assay, we conducted an 8000-compound  
273 pilot screen and identified several compounds that inhibit the basal GTPase activity of  
274 Dyn1. The commercially available dynamin inhibitors, Dynasore and Dyngo-4a, were  
275 tested for their ability to inhibit dynamin's basal GTPase activity in the Transcreener  
276 assay format. Although both Dynasore and Dyngo-4a could inhibit the NT-stimulated  
277 GTPase activity of Dyn1, neither was able to inhibit basal GTPase activity in our hands.  
278 Moreover, the reported IC<sub>50</sub> values we measured for Dynasore and Dyngo-4a NT-  
279 stimulated GTPase activity performed at physiological salt concentrations using 100 nM  
280 dynamin were much higher than those reported for assays performed in the presence of  
281 sonicated PS liposomes, under low salt conditions with 20 nM dynamin (0.4 μM and 12

282  $\mu\text{M}$ , respectively). Given the reported off-target effects of Dynasore and Dyngo-4a [16-  
283 18] and their uncertain mechanism of dynamin inhibition, a more robust and specific  
284 inhibitor of dynamin would be of immense value.

285 As with any assay, fluorescence polarization has its limitations. Compounds that  
286 are either auto-fluorescent, or affect the affinity of the anti-GDP antibody for the tracer  
287 may be misinterpreted as potential hits [20]. The hits must therefore be validated in  
288 secondary assays such as the malachite green assay and eventually for their ability to  
289 inhibit dynamin-dependent, clathrin-mediated endocytosis in intact cells.

290 Having validated our assay using an 8000-compound pilot screen, we are  
291 currently expanding our search for robust, specific, and cell-permeable dynamin  
292 inhibitors by screening the entire UT Southwestern chemical library of 230,000  
293 compounds using the optimized Transcreeper GDP FP assay.

294

## 295 **Acknowledgements**

296 We thank Dana K. Reed for helping with protein expression and purification. We  
297 also thank the members of the Schmid lab for thoughtful discussions.

298

## 299 **References**

- 300 1. Ferguson SM, De Camilli P. Dynamin, a membrane-remodelling GTPase. *Nat*  
301 *Rev Mol Cell Biol.* 2012;13(2):75-88.
- 302 2. Morlot S, Roux A. Mechanics of dynamin-mediated membrane fission. *Annu Rev*  
303 *Biophys.* 2013;42:629-49.

- 304 3. Schmid SL, Frolov VA. Dynamin: functional design of a membrane fission  
305 catalyst. *Annu Rev Cell Dev Biol.* 2011;27:79-105.
- 306 4. Shupliakov O, Low P, Grabs D, Gad H, Chen H, David C, et al. Synaptic vesicle  
307 endocytosis impaired by disruption of dynamin-SH3 domain interactions. *Science.*  
308 1997;276(5310):259-63.
- 309 5. Loerke D, Mettlen M, Yarar D, Jaqaman K, Jaqaman H, Danuser G, et al. Cargo  
310 and dynamin regulate clathrin-coated pit maturation. *PLoS Biol.* 2009;7(3):e57.
- 311 6. Reis CR, Chen PH, Srinivasan S, Aguet F, Mettlen M, Schmid SL. Crosstalk  
312 between Akt/GSK3beta signaling and dynamin-1 regulates clathrin-mediated  
313 endocytosis. *EMBO J.* 2015;34(16):2132-46.
- 314 7. Sever S, Damke H, Schmid SL. Dynamin:GTP controls the formation of  
315 constricted coated pits, the rate limiting step in clathrin-mediated endocytosis. *J Cell*  
316 *Biol.* 2000;150(5):1137-48.
- 317 8. Song BD, Schmid SL. A molecular motor or a regulator? Dynamin's in a class of  
318 its own. *Biochemistry.* 2003;42(6):1369-76.
- 319 9. Chappie JS, Acharya S, Leonard M, Schmid SL, Dyda F. G domain dimerization  
320 controls dynamin's assembly-stimulated GTPase activity. *Nature.* 2010;465(7297):435-  
321 40.
- 322 10. Stowell MH, Marks B, Wigge P, McMahon HT. Nucleotide-dependent  
323 conformational changes in dynamin: evidence for a mechanochemical molecular spring.  
324 *Nat Cell Biol.* 1999;1(1):27-32.

- 325 11. Barylko B, Binns D, Lin KM, Atkinson MA, Jameson DM, Yin HL, et al.  
326 Synergistic activation of dynamin GTPase by Grb2 and phosphoinositides. *J Biol Chem.*  
327 1998;273(6):3791-7.
- 328 12. Gout I, Dhand R, Hiles ID, Fry MJ, Panayotou G, Das P, et al. The GTPase  
329 dynamin binds to and is activated by a subset of SH3 domains. *Cell.* 1993;75(1):25-36.
- 330 13. Warnock DE, Hinshaw JE, Schmid SL. Dynamin self-assembly stimulates its  
331 GTPase activity. *J Biol Chem.* 1996;271(37):22310-4.
- 332 14. Macia E, Ehrlich M, Massol R, Boucrot E, Brunner C, Kirchhausen T. Dynasore,  
333 a cell-permeable inhibitor of dynamin. *Dev Cell.* 2006;10(6):839-50.
- 334 15. McCluskey A, Daniel JA, Hadzic G, Chau N, Clayton EL, Mariana A, et al.  
335 Building a better dynasore: the dyngo compounds potently inhibit dynamin and  
336 endocytosis. *Traffic.* 2013;14(12):1272-89.
- 337 16. Park RJ, Shen H, Liu L, Liu X, Ferguson SM, De Camilli P. Dynamin triple  
338 knockout cells reveal off target effects of commonly used dynamin inhibitors. *J Cell Sci.*  
339 2013;126(Pt 22):5305-12.
- 340 17. Preta G, Cronin JG, Sheldon IM. Dynasore - not just a dynamin inhibitor. *Cell*  
341 *Commun Signal.* 2015;13:24.
- 342 18. Basagiannis D, Zografou S, Galanopoulou K, Christoforidis S. Dynasore impairs  
343 VEGFR2 signalling in an endocytosis-independent manner. *Sci Rep.* 2017;7:45035.
- 344 19. Neumann S, Schmid SL. Dual role of BAR domain-containing proteins in  
345 regulating vesicle release catalyzed by the GTPase, dynamin-2. *J Biol Chem.*  
346 2013;288(35):25119-28.



- 347 20. Sun W, Vanhooke JL, Sondek J, Zhang Q. High-throughput fluorescence  
348 polarization assay for the enzymatic activity of GTPase-activating protein of ADP-  
349 ribosylation factor (ARFGAP). *J Biomol Screen*. 2011;16(7):717-23.
- 350 21. Wu Z, Liu D, Sui Y. Quantitative assessment of hit detection and confirmation in  
351 single and duplicate high-throughput screenings. *J Biomol Screen*. 2008;13(2):159-67.
- 352 22. Leonard M, Song BD, Ramachandran R, Schmid SL. Robust colorimetric assays  
353 for dynamin's basal and stimulated GTPase activities. *Methods Enzymol*. 2005;404:490-  
354 503.
- 355 23. Lea WA, Simeonov A. Fluorescence polarization assays in small molecule  
356 screening. *Expert Opin Drug Discov*. 2011;6(1):17-32.
- 357 24. Liu YW, Mattila JP, Schmid SL. Dynamin-catalyzed membrane fission requires  
358 coordinated GTP hydrolysis. *PLoS One*. 2013;8(1):e55691.
- 359

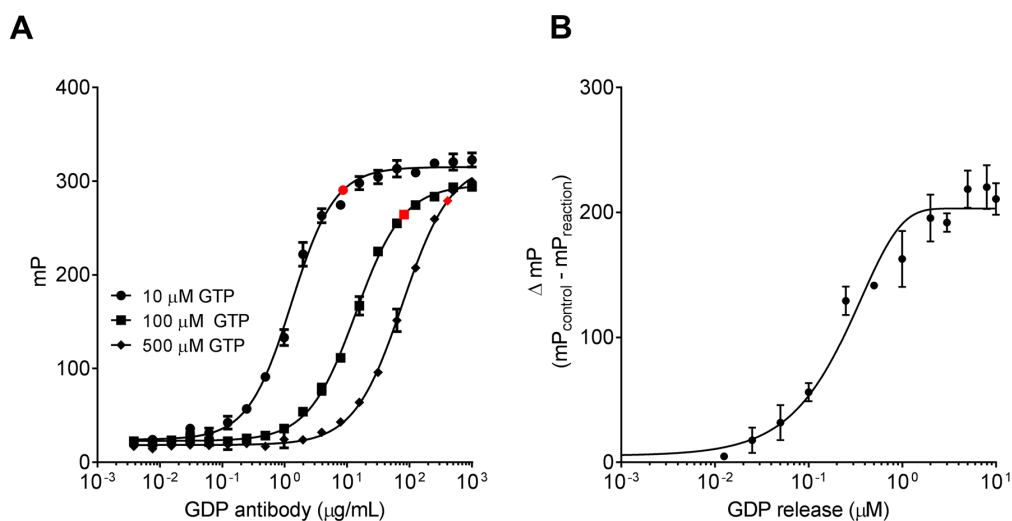


**Fig 1. Optimization of assay sensitivity to measure GDP production**

**A)** The GDP antibody was titrated to determine its optimal concentrations for 10, 100 and 500  $\mu\text{M}$  GTP. Optimal antibody concentrations are represented by the highlighted points ( $n = 1$ , measured in triplicates). **B)** Standard curve representing the conversion of 0 to 100% GDP from 10  $\mu\text{M}$  GTP. This curve was used to convert the fluorescence polarization data to GDP released ( $n = 1$ , measured in triplicates). Data are presented as mean  $\pm$  SD.

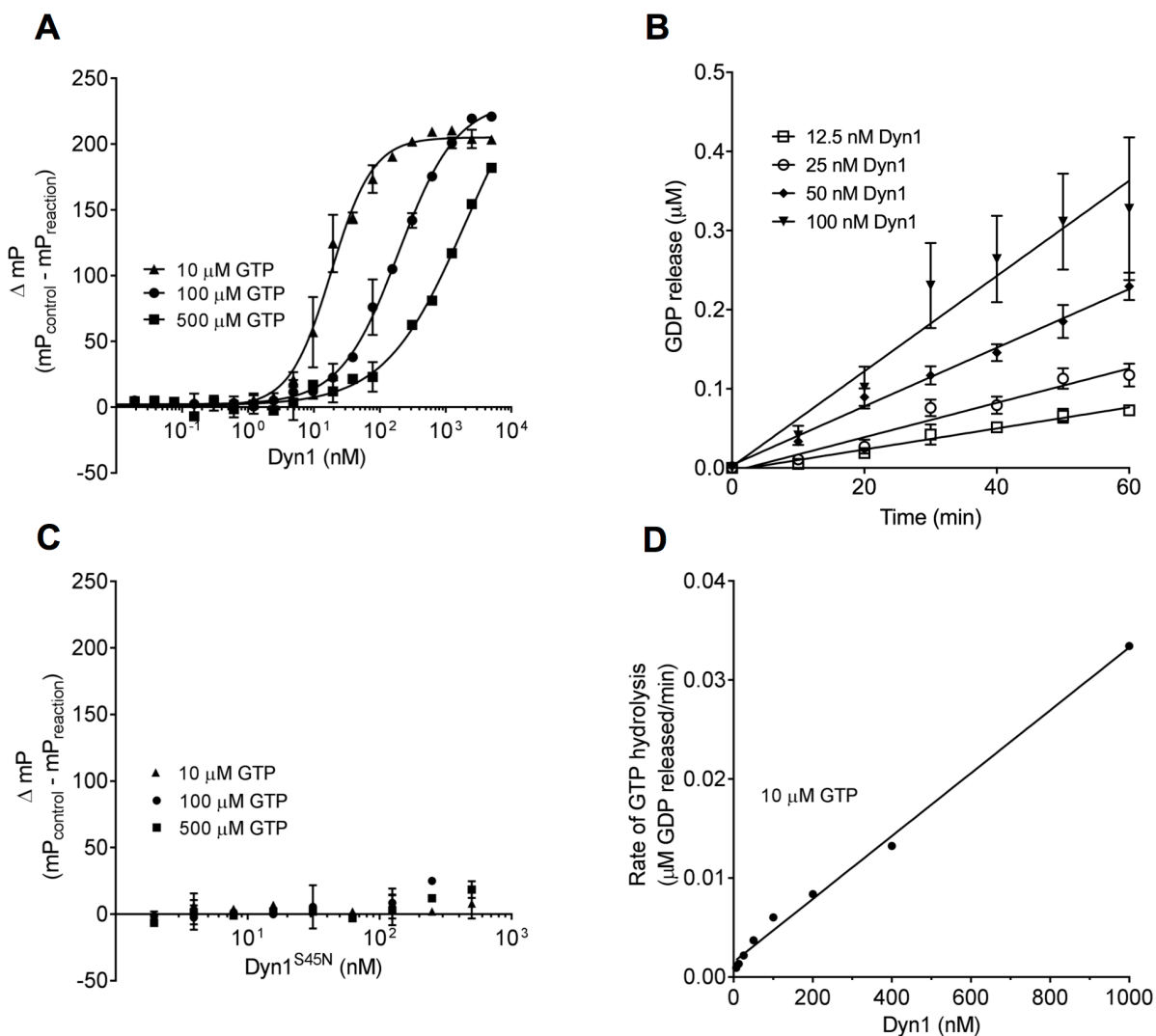


**Fig 2. Detection of basal GTP hydrolysis by Dyn1**

**A)** Dyn1 was titrated from 0.3 nM to 5000 nM in the presence of 10  $\mu$ M, 100  $\mu$ M or 500  $\mu$ M GTP and GTP hydrolysis was measured as  $\Delta$ mP after 60 min incubation at room temperature (n = 1, measured in triplicates). **B)** The GTP hydrolysis by Dyn1 was linear during 60 minute incubations at room temperature (n = 4, each measured in duplicates). **C)** The GTP binding mutant, Dyn1<sup>S45N</sup>, shows no activity at any concentration of GTP (n = 1, measured in triplicates). **D)** The basal GTPase activity is proportional to Dyn1 concentration from 0 to 1000 nM, indicating no cooperativity under these concentrations (n = 3, each measured in triplicates). Data are presented as mean  $\pm$  SD.

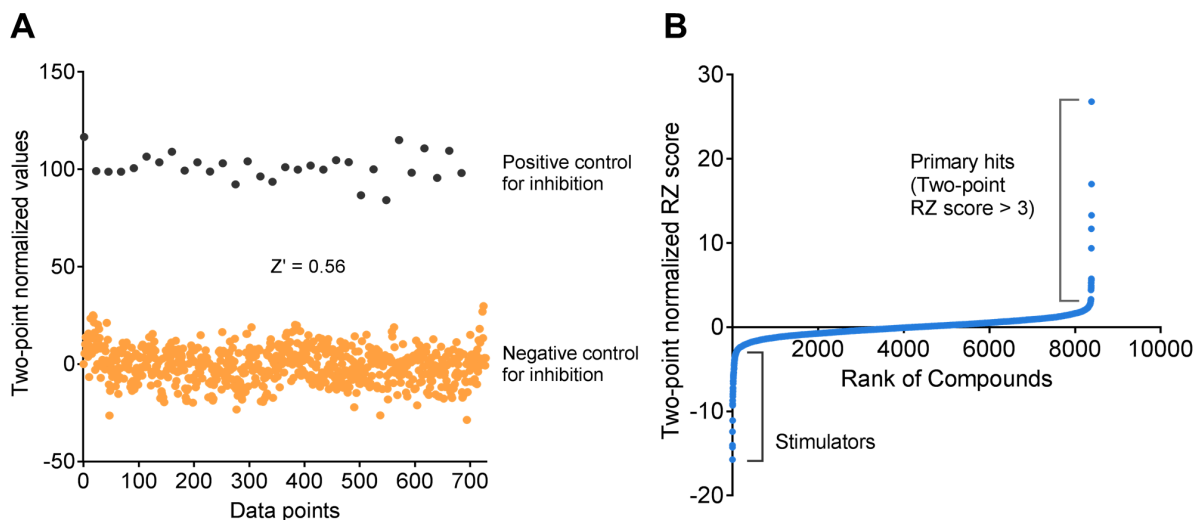


**Fig 3. Assay validation and application for high-throughput screening of 8000 compounds.**

**A)** The assay was validated in a preliminary mock screen that compared reactions containing no enzyme (positive control for inhibition) to uninhibited reactions containing DMSO (negative control for inhibition). **B)** A quantile-quantile (Q-Q) plot of the pilot screen of 8000 compounds. The compounds are ranked from 0 to 8000 according to their two-point robust Z score. Primary hits were chosen based on a RZ score of greater than 3.

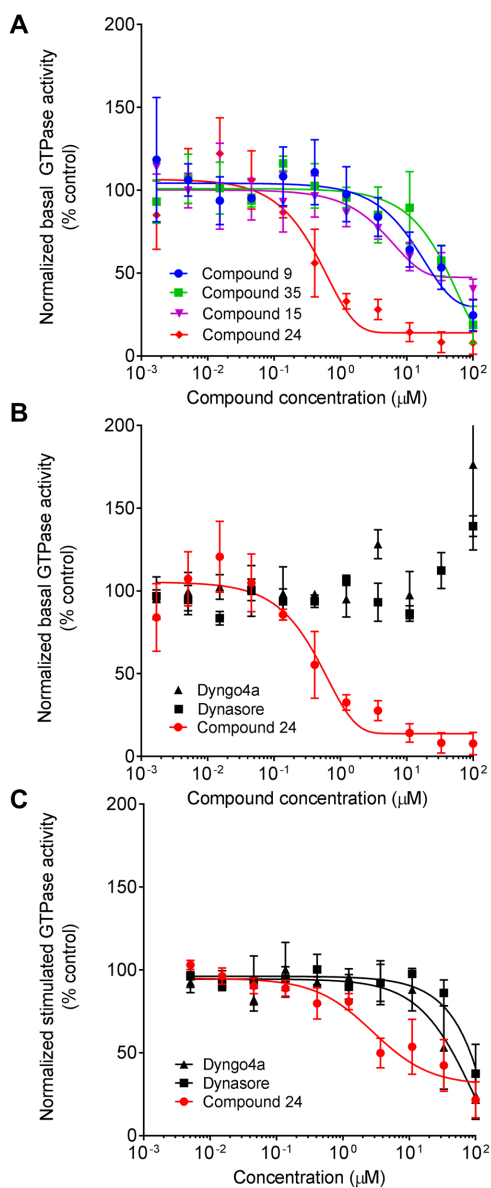


**Fig 4. Comparison of commercially available inhibitors with compound 24**

**A)** 11-point dose response curve of the 4 validated hits from the primary screen of 8000 compounds measured using 50 nM Dyn1 and 10  $\mu\text{M}$  GTP ( $n = 1$ , measured in triplicates). **B)** Dynasore and Dyngo-4a were tested alongside compound 24 in the Transcreeper assay ( $n = 1$ , measured in triplicates). **C)** Dose response curves for the inhibitory effects of Dynasore, Dyngo-4a and compound 24 on the lipid nanotube-stimulated GTPase activity of 100 nM Dyn1 assayed in the presence of 300  $\mu\text{M}$  lipid nanotubes and 25  $\mu\text{M}$  GTP and measured using the malachite green assay ( $n = 3$ , each measured in triplicates). Data are presented as mean  $\pm$  SD.